

# Secure Spatial Signal Design for ISAC in a Cell-Free MIMO Network

Steven Rivetti, Emil Björnson, Mikael Skoglund,

School of Electrical Engineering and Computer Science (EECS), KTH Royal Institute of Technology, Sweden

**Abstract**—In this paper, we study a cell-free multiple-input multiple-output network equipped with integrated sensing and communication (ISAC) access points (APs). The distributed APs are used to jointly serve the communication needs of user equipments (UEs) while sensing a target, assumed to be an eavesdropper (Eve). To increase the system’s robustness towards said Eve, we develop an ISAC waveform model that includes artificial noise (AN) aimed at degrading the Eve channel quality. The central processing unit receives the observations from each AP and calculates the optimal precoding and AN covariance matrices by solving a semi-definite relaxation of a constrained Cramer-Rao bound (CRB) minimization problem. Simulation results highlight an underlying trade-off between sensing and communication performances: in particular, the UEs signal-to-noise and interference ratio and the maximum Eve’s signal to noise ratio are directly proportional to the CRB. Furthermore, the optimal AN covariance matrix is rank-1 and has a peak in the eve’s direction, leading to a surprising inverse-proportionality between the UEs-Eve distance and optimal-CRB magnitude.

**Index Terms**—Cell-free MIMO, ISAC, CRB, signal design.

## I. INTRODUCTION

6G networks and other future communication systems are expected to include sensing functionalities as a fundamental component [1]. Assuming an efficient sharing of hardware and wireless resources, the communication infrastructure can have low-cost sensing capabilities and the sensing frequency bands can be used for wireless communications. To do that, however, the integrated sensing and communications (ISAC) system’s different components, including the transmission waveform, received data post-processing and the multiple-input multiple-output (MIMO) beamforming must be carefully co-designed. The single ISAC access point (AP) case has been the main focus of earlier studies [2]. In reality, however, numerous ISAC APs will operate in the same area, frequency range, and period of time, thus creating interference between each other. This encourages these dispersed APs to work together to enhance their performance and mitigate the aforementioned interference [3]. Because of the shared usage of the spectrum and the broadcasting nature of wireless transmission, ISAC systems’ security is facing several challenges. On the one hand, Rician channels, which are frequently occurring at mmWave frequencies and contain a line of sight (LoS) component, are inextricably linked to the sensing channel. This differs from traditional physical layer security (PLS) research [4] in communication systems with the premise that the legitimate user channels and intercept channels are independently and identically distributed. The confidential information designated to the user equipments (UEs) is included

in the dual-functional waveform, namely a waveform that jointly serves the communication UEs and senses the sensing target [5], and is therefore vulnerable to being intercepted by the sensing target. Reasons for implementing such safety measures can stem from various factors. For instance, in scenarios involving vehicle tracking for safety purposes, it is essential to enable vehicle monitoring while preventing unauthorized access to the ongoing communication. Let us consider a communication network deployed in an open-air industrial area, where incoming vehicles deliver goods. The system aims to track the vehicles autonomously, avoiding accidents, and simultaneously safeguarding the confidentiality of the data traffic to prevent industrial espionage.

From the sensing side, a crucial and intriguing trade-off appears: the power is expected to be directed towards the sensing target, however, the useful signal information must be protected from being intercepted by said target, who is identified as a malicious agent. On the other hand, regardless of the sensing target’s actions and intentions, it is important to increase the system’s estimation and detection performance. In conventional communication systems, security issues are addressed at the higher levels of the protocol stack with cryptographic techniques [6], even though it is worth mentioning that studies on cryptography frequently assume that the physical layer provides a link that is error-free, but in reality, wireless communications are subject to assaults, increasing the risk of information loss.

### A. Related work

In [7], the authors consider a cell-free MIMO network equipped with ISAC APs and devise a transmit waveform co-design strategy aimed at maximizing the signal to noise ratio (SNR) of the sensing target, here assumed to be a benign agent, under a minimum signal to noise and interference ratio (SINR) constraint for the communication users. The performance of this transmit strategy, in terms of achieved communication SINR and sensing SNR, are compared against well-established sensing-prioritized and communication-prioritized design strategies, demonstrating the performance gain achieved by the proposed co-design strategy. On the other hand, in [8], the idea of adding artificial noise (AN) to the transmitted waveform to improve the network PLS is introduced. This technique is an alternative to coding-based schemes aimed at achieving the same goal [9]. This work considers a single AP with multiple targets, assumed to be eavesdroppers (Eves), and derives the optimal beamforming

strategy by solving a weighted optimization problem. The objective functions bound together by the weighted optimization are the Cramer-Rao bound (CRB) onto the targets' angles and the system's secrecy rate, defined as the minimum difference between each user's achievable rate and a sensing rate, defined as  $\log_2(1 + \text{SNR})$ .

### B. Contributions

Contrary to the existing literature, this paper investigates how AN can be used by distributed ISAC APs, cooperating to increase the PLS of a cell-free MIMO network. Said network is made of  $M$  APs that serve multiple communication users and simultaneously sensing a target, assumed to be an Eve, using the same signal. In addition to its monostatic observation, every AP receives the reflected echos from all the other APs and sends them to a central processing unit (CPU) through a back-haul link here assumed error-free.

The main contributions of this paper are the following:

- We propose a novel transmit waveform model to be used by distributed ISAC APs in a cell-free MIMO network.
- We calculate the optimal transmit waveform by solving a constrained CRB minimization problem. The relaxed version of the original problem is proved to be tight for the scenario at hand
- We characterize the optimal AN structure, showing that it's rank-1 and directed towards the eve.
- Numerical simulation prove the trade-off between sensing and communication performances and show the effects that the UEs-Eve proximity has on the optimal CRB.

## II. SYSTEM MODEL

Consider a cell-free MIMO network consisting of  $M$  APs,  $K$  UEs and a sensing target, assumed to be an eve. To protect the privacy and security of the data traffic from the eve, we introduce an AN vector  $\xi$  [8] that will be used to reduce the sensing target's SNR. Each AP is equipped with a uniform linear array (ULA) comprising  $N$  transmit and  $N$  receive antennas.

The inter-element spacing within the ULA is set to  $\lambda/2$ , where  $\lambda$  is the carrier wavelength. Conversely, each UE is equipped with a single antenna. Digital beamforming capabilities are assumed for each AP, which is connected to a CPU responsible for designing the transmit signals. In each timeslot  $t$ , AP  $m$  transmits a waveform denoted by the complex vector  $\phi_m^t \in \mathbb{C}^N$ , which can be modeled as

$$\phi_m^t = \sum_{s=1}^S \mathbf{f}_{m,s} x_{m,s}^t + \xi_m^t, \quad (1)$$

where  $\mathbf{f}_{m,s} \in \mathbb{C}^N$  is the precoding vector used by AP  $m$  for stream  $s$ .  $S$  represents the number of transmission streams: each UE is served by one transmission stream and an additional stream is allocated for sensing purposes. Consequently,  $S = K + 1$ . On the other hand,  $x_{m,s}^t$  represents the complex-valued unitary-power information symbol and the vector  $\xi_m^t \in \mathbb{C}^N$  represents the AN vector transmitted during timeslot

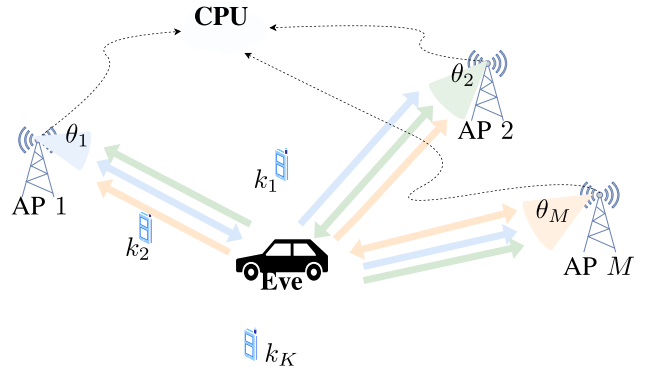


Fig. 1: illustration of the Cell-free MIMO network where ISAC APs serve communication users while sensing an Eve

$t$  by AP  $m$ . This noise is statistically independent of the transmitted symbols. In order to maximize its entropy, said noise is modeled as a complex Gaussian distributed vector with zero mean and covariance matrix  $\mathbf{R}_{\xi_m}$ . We can get rid of the summation and express (1) using matrices:

$$\phi_m^t = \mathbf{F}_m \mathbf{x}_m^t + \xi_m^t, \quad (2)$$

where  $\mathbf{F}_m = [\mathbf{f}_{m,1} \dots \mathbf{f}_{m,S}] \in \mathbb{C}^{N \times S}$  and  $\mathbf{x}_m^t = [x_{m,1}^t \dots x_{m,S}^t]^\top \in \mathbb{C}^S$ . All the following derivations assume that symbols belonging to different streams and different APs are statistically uncorrelated, i.e.,  $\mathbb{E}[(x_{m,s}^t)^H (x_{m',s'}^t)] = 1$  if and only if  $m = m'$  and  $s = s'$ . This condition can be achieved through pseudo-random coding [10].

### A. Communication observation

The channel vector between UE  $u$  and AP  $m$  is denoted by the vector  $\mathbf{h}_{m,k} \in \mathbb{C}^N$ . This allows us to define the received signal observed by UE  $k$  during the timeslot  $t$  as

$$y_{k,t}^c = \sum_{m=1}^M \mathbf{h}_{m,k}^H \phi_m^t + w_u = \sum_{m=1}^M \mathbf{h}_{m,k}^H \mathbf{f}_{m,k} x_{m,k}^t + \sum_{s=1}^S \sum_{m=1}^M \mathbf{h}_{m,k}^H \mathbf{f}_{m,s} x_{m,s}^t + \sum_{m=1}^M \mathbf{h}_{m,k}^H \xi_m^t + w_k, \quad (3)$$

where  $w_k \sim \mathcal{CN}(0, \sigma_c^2)$  is the receiver noise, assumed to be uncorrelated from the transmitted waveform.

### B. Multistatic sensing

As shown in Fig. 1, the APs implement multistatic sensing: every AP receives the echo of its own transmitted signal plus the reflections coming from all of the other APs. The Eve is modeled as a point reflector having a LoS path with every AP.

Under these assumptions, we can define the radar observations collected by AP  $m$  during timeslot  $t$  as [7]

$$\begin{aligned} \mathbf{y}_{m,t}^s &= \sum_{s=1}^S \sum_{m'=1}^M \underbrace{\alpha_{m'}^m \mathbf{a}(\theta_m) \mathbf{a}(\theta_{m'})^H \phi_{m',s}^t}_{\mathbf{g}_{m,s}^t} + \mathbf{n}_m \\ &= \sum_{s=1}^S \sum_{m'=1}^M \alpha_{m'}^m \mathbf{a}(\theta_m) \mathbf{a}(\theta_{m'})^H \mathbf{f}_{m',s} x_{m',s}^t \\ &\quad + \sum_{s=1}^S \sum_{m'=1}^M \alpha_{m'}^m \mathbf{a}(\theta_m) \mathbf{a}(\theta_{m'})^H \boldsymbol{\xi}_{m'}^t + \mathbf{n}_m, \end{aligned} \quad (4)$$

where  $|\alpha_{m'}^m|^2$  is the channel gain between the transmitting AP  $m'$  and receiving AP  $m$ . To take into account the effects of pathloss and radar cross section (RCS), the channel gain is modeled according to the Swerling-I model, that is  $\alpha_{m'}^m \sim \mathcal{CN}(0, (\delta_{m'}^m)^2)$ . The angles  $\theta_m$  and  $\theta_{m'}$  represent the angle of arrival (AoA) to AP  $m$  and the angle of departure (AoD) from AP  $m'$ , whereas  $\mathbf{a}(\cdot)$  is the steering vector of a ULA. The thermal noise vector is denoted by  $\mathbf{n}_m \sim \mathcal{CN}(0, \sigma_s^2 \mathbf{I}_N)$ , and is assumed to be uncorrelated from the transmitted waveform.

### III. TRANSMITTED WAVEFORM JOINT DESIGN

The sensing objective we have chosen to minimize is the CRB on  $\theta_1, \dots, \theta_m$ . Assuming that the optimal waveform is computed during timeslot  $t$ , we assume that  $\theta_1, \dots, \theta_m$  have been estimated (e.g. using the MUSIC algorithm with omnidirectional pilots [11]) during timeslot  $t-1$  and that, given a low mobility of the Eve, said estimations still hold true during the present timeslot. In this way, using the initial estimation, The cell-free MIMO network can compute a transmit waveform that boosts its future estimation performances while simultaneously degrading the Eve channel quality by means of the AN. In this section, we first derive the Fisher information matrix (FIM) and CRB and then use them to define the optimization problem through which we design the optimal transmitted waveform, semi-definite relaxation (SDR) is used to obtain a relaxed problem solvable through complex optimization solvers.

#### A. CRB derivation

Let  $\boldsymbol{\eta} \in \mathbb{R}^{(2M^2+M)}$  denote the vector of unknown channel parameters

$$\boldsymbol{\eta} = [\Re\{\alpha_1^1\}, \Im\{\alpha_1^1\}, \dots, \Re\{\alpha_M^M\}, \Im\{\alpha_M^M\}, \theta_1, \dots, \theta_M]^\top, \quad (5)$$

where  $\Re\{\alpha_1^1\}$  and  $\Im\{\alpha_1^1\}$  represent the real and imaginary part of the complex channel coefficient  $\alpha_1^1$ . Let us then define the vectors  $\mathbf{y}_t^s = [\mathbf{y}_{1,t}^s \dots \mathbf{y}_{M,t}^s]^\top \in \mathbb{C}^{M \times N}$

and  $\mathbf{g}_s^t = [\mathbf{g}_{1,s}^t \dots \mathbf{g}_{M,s}^t]^\top \in \mathbb{C}^{M \times N}$ . The FIM  $\mathbf{J}_\boldsymbol{\eta} \in \mathbb{R}^{(2M^2+M) \times (2M^2+M)}$  can be then calculated as

$$\begin{aligned} \mathbf{J}_\boldsymbol{\eta} &= \mathbb{E}_{\mathbf{y}_t^s | \boldsymbol{\eta}} \left[ - \frac{\partial^2 \log f(\mathbf{y}_t^s | \boldsymbol{\eta})}{\partial \boldsymbol{\eta} \partial \boldsymbol{\eta}^\top} \right] \\ &= \frac{2}{\sigma_s^2} \sum_{s=1}^S \Re \left\{ \left( \frac{\partial \mathbf{g}_s^t}{\partial \boldsymbol{\eta}} \right)^H \left( \frac{\partial \mathbf{g}_s^t}{\partial \boldsymbol{\eta}} \right) \right\}, \end{aligned} \quad (6)$$

where  $f(\mathbf{y}_t^r | \boldsymbol{\eta})$  is the conditional likelihood function of the stacked observation vector  $\mathbf{y}_t^r$  given  $\boldsymbol{\eta}$ . The CRB for the estimation of  $\theta_m$  is then defined as

$$\text{CRB}_{\theta_m} = \sqrt{[\mathbf{J}_\boldsymbol{\eta}^{-1}]_{2M^2+m, 2M^2+m}}. \quad (7)$$

The square root has been included to facilitate future comparison with the estimation root mean square error.

#### B. Optimal transmit waveform

The chosen optimization metric is practically translated into the minimization of the FIM's inverse trace. The optimization variables are the AP precoding matrices  $\mathbf{F}_m$  and the AN covariance matrices  $\mathbf{R}_{\Xi_m}$ . In order to define the constraints of the optimization problem, we first need to mathematically define the UE SINR and the Eve SNR. The communication channel  $\mathbf{h}_{m,k}$  is assumed to be deterministic, a condition achievable through the acquisition of channel-state information at the transmitter, and the multi-user interference is treated as noise [7]. Following (3), the SINR for user  $k$  can be defined as

$$\begin{aligned} \text{SINR}_k &= \frac{\sum_{m=1}^M |\mathbf{h}_{m,k}^H \mathbf{f}_{m,k}|^2}{\sum_{m=1}^M \sum_{s \neq k}^S |\mathbf{h}_{m,k}^H \mathbf{f}_{m,s}|^2 + \sum_{m=1}^M |\mathbf{h}_{m,k}^H \mathbf{R}_{\Xi_m} \mathbf{h}_{m,k}| + \sigma_c^2}. \end{aligned} \quad (8)$$

On the other hand, the eve's SNR can be modelled as

$$\text{SNR}_E = \frac{\sum_{m=1}^M \sum_{s=1}^S (\delta_m^m)^2 |\mathbf{a}(\theta_m)^H \mathbf{f}_{s,m}|^2}{\sum_{m=1}^M (\delta_m^m)^2 |\mathbf{a}(\theta_m)^H \mathbf{R}_{\Xi_m} \mathbf{a}(\theta_m)| + \sigma_s^2}. \quad (9)$$

We are now able to define the proposed transmit waveform design strategy

$$\begin{aligned} \min_{\{\mathbf{R}_{\Xi_m}\}_1^M, \{\mathbf{f}_{m,s}\}_{1,1}^{M,S}} & \text{Tr}(\mathbf{J}_\boldsymbol{\eta}^{-1}), & (10a) \\ \text{s.t.} & \text{SINR}_k \geq \gamma_k, \quad k = 1, \dots, K & (10b) \\ & \text{SNR}_E \leq \psi, & (10c) \\ & \|\phi_t\|^2 \leq P_m, \quad m = 1 \dots M, & (10d) \end{aligned}$$

where  $P_m, \gamma_k$  and  $\psi$  represent the available power at AP  $m$ , the required SINR for user  $k$ , and the maximum SNR that the Eve should be allowed to achieve.

#### C. Semidefinite reformulation

Problem (10) is non-convex in the variable  $\mathbf{f}_{m,s}$  due to the quadratic terms occurring in both the SINR and SNR. To solve this, we reformulate (10) as an semi-definite program (SDP)[12]. In particular, we define the variable  $\mathbf{W}_s = \mathbf{f}_s \mathbf{f}_s^H$ , where  $\mathbf{f}_s = [\mathbf{f}_{1,s}^\top \dots \mathbf{f}_{M,s}^\top]^\top \in \mathbb{C}^{NM}$  and express the objective

function and the constraints as a function of this variable. We can then reformulate (10b) as

$$\begin{aligned} \text{Tr}(\mathbf{h}_k \mathbf{h}_k^H \mathbf{W}_k) &\geq \\ \gamma_k \left( \sum_{\substack{s \neq k \\ s=1}}^S \text{Tr}(\mathbf{h}_k \mathbf{h}_k^H \mathbf{W}_s) + \sum_{m=1}^M \text{Tr}(\mathbf{h}_{m,k} \mathbf{h}_{m,k}^H \mathbf{R}_{\Xi_m}) + \sigma_c^2 \right), \end{aligned} \quad (11)$$

where  $\mathbf{h}_k = [\mathbf{h}_{1,k}^\top \dots \mathbf{h}_{M,k}^\top]^\top \in \mathbb{C}^{NM}$ . Similarly, the Eve's SNR constraint in (10c) can be redefined as

$$\begin{aligned} \sum_{m=1}^M \sum_{s=1}^S (\delta_m^m)^2 \text{Tr}(\mathbf{a}(\theta_m) \mathbf{a}(\theta_m)^H \mathbf{W}_{m,s}) &\leq \\ \psi \left( \sum_{m=1}^M (\delta_m^m)^2 \text{Tr}(\mathbf{a}(\theta_m) \mathbf{a}(\theta_m)^H \mathbf{R}_{\Xi_m}) + \sigma_s^2 \right), \end{aligned} \quad (12)$$

where  $\mathbf{W}_{m,s} = \mathbf{f}_{m,s} \mathbf{f}_{m,s}^H$  and this is the  $m^{\text{th}}$   $N \times N$  block onto the main diagonal of  $\mathbf{W}_s$ . Leveraging the lack of correlation between the terms in (2), (10d) can be re-written as:

$$\|\phi_m^t\|^2 = \text{Tr} \left( \sum_{s=1}^S \mathbf{W}_{m,s} + \mathbf{R}_{\Xi_m} \right) \leq P_m. \quad (13)$$

Eventually, the SDP-equivalent problem can be defined as :

$$\min_{\{\mathbf{R}_{\Xi_m}\}_1^M, \{\mathbf{W}_s\}_1^S} \text{Tr}(\mathbf{J}_\eta^{-1}) \quad (14a)$$

$$\text{s.t. (11) } k = 1 \dots K, \quad (14b)$$

$$(12) \quad (14c)$$

$$(13) m = 1 \dots M, \quad (14d)$$

$$\text{rank}(\mathbf{W}_s) = 1, \quad s = 1 \dots S \quad (14e)$$

$$\mathbf{W}_s \in \mathbb{S}^+, \quad s = 1 \dots S, \quad (14f)$$

where  $\mathbb{S}^+$  represents the set of Hermitian positive semidefinite matrices, the reformulation of  $\mathbf{J}_\eta$  elements as a function of the relaxed variables is shown in the appendix. This problem can be relaxed by removing constraint (14e) and then solved via convex optimization solvers [13]:

$$\min_{\{\mathbf{R}_{\Xi_m}\}_1^M, \{\mathbf{W}_s\}_1^S} \text{Tr}(\mathbf{J}_\eta^{-1}) \quad (15a)$$

$$\text{s.t. (11) } k = 1 \dots K, \quad (15b)$$

$$(12) \quad (15c)$$

$$(13) m = 1 \dots M, \quad (15d)$$

$$\mathbf{W}_s \in \mathbb{S}^+, \quad s = 1 \dots S. \quad (15e)$$

In the next section we show that the optimal solution of problem 15 yields rank-1 matrices, making said solution optimal for problem 14 and the relaxation tight.

#### IV. SIMULATION RESULTS

In this section, we now present the performance of the proposed waveform design strategy in a cell-free MIMO network with  $M = 2$  APs, each of them equipped with a ULA of  $N = 30$  antennas, using the same waveform to serve  $K = 4$  UEs and sense one Eve. The UEs are randomly

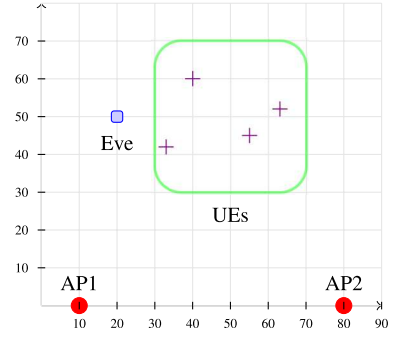


Fig. 2: simulated APs and UEs layout, the UEs are randomly placed within the green box

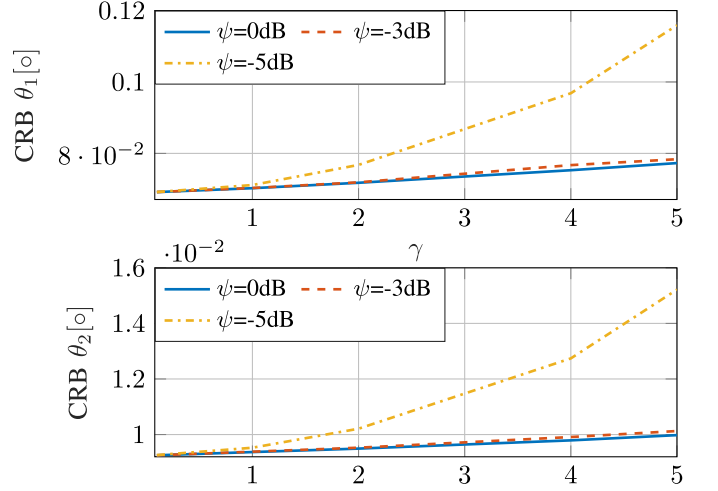


Fig. 3: AP 1 (top) and AP 2 (bottom) CRB on  $\theta_m$  for different  $\psi$

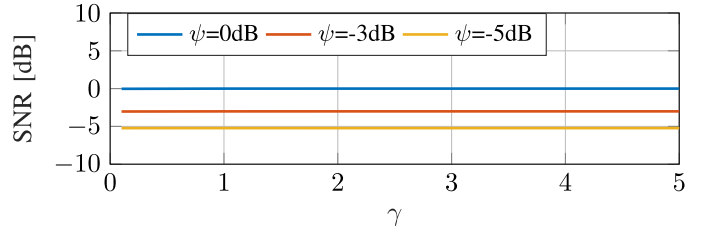


Fig. 4: achieved eve's SNR vs  $\gamma$  for different values of  $\psi$

distributed in a  $40 \times 40$  m area in front of the APs, located at the coordinates  $[10, 0]$  and  $[80, 0]$ . We then choose  $P_m = 1$  W the noise variances are  $\sigma_c^2 = \sigma_s^2 = 1$ . The Swerling-I model variance  $(\delta_{m'}^m)^2$  has been set to 0.1 for all the  $m, m'$  pairs. Unless otherwise specified, the maximum  $\psi$  has been set to 0 dB. All the UEs are envisioned to be guaranteed the same SINR, thus  $\gamma_1 = \dots = \gamma_K = \gamma$

##### A. CRB dependency by $\psi$

In this subsection we investigate how the choice of  $\psi$  affects the achieved CRB on  $\theta_1$  and  $\theta_2$ . Fig. 3 shows the achieved CRB as a function of  $\gamma$  for three different  $\psi$ : We observe that larger  $\gamma$  values correspond to higher CRB values. This

is a manifestation of the sensing-communication trade-off: as the SINR requirements become more demanding, the system needs to allocate more resources on the communication side, thus degrading the sensing performances, namely achieving a higher CRB. A second trade-off arises between the CRB and  $\psi$ : a more stringent constraint onto the Eve's SNR corresponds to worse sensing performances. This can be ascribed to the direct proportionality between the system's sensing capabilities, namely the CRB, and the amount of power beamformed towards the target, i.e. the SNR. Fig. 3 shows that constraining the sensing SNR to  $\psi = -5$  dB cause sensibly higher CRB than the case where  $\psi = 0$  dB, whereas setting  $\psi = -3$  dB generates a CRB very similar to the former. This implies that a 3 dB decrease of the allowed sensing SNR, i.e. from 0 dB to  $-3$ dB, cause a very little degradation in the sensing performance and thus the latter is preferable to the former. Fig. 4 indicates that constraint (12) is tight as the achieved Eve's SNR is equal to  $\psi$

### B. Relaxation's tightness

The optimal  $\mathbf{W}_s$  for the communication streams (i.e.  $s = 1 \dots K$ ) are all rank-1 matrices. The communication beamforming vectors can be retrieved as

$$\begin{aligned} \mathbf{f}_{s,m} &= [\sqrt{\epsilon_s} \mathbf{u}]_{(m-1)N+1 : mN}, \\ m &= 1 \dots M, \quad s = 1 \dots K, \end{aligned} \quad (16)$$

where  $\epsilon_k$  and  $\mathbf{u}$  are the non-zero eigenvalue and respective eigenvector associated to  $\mathbf{W}_s$ . As for the sensing stream (i.e.  $s = K + 1$ ) The optimal  $\mathbf{W}_s$  is not rank-1 as all its eigenvalues are in the order of  $10^{-5}$ : We can then say that  $\mathbf{W}_s$  has rank-almost zero, making the presence of a sensing stream superfluous. Lastly, the The optimal AN covariance matrices  $\{\mathbf{R}_{\Xi_m}^{\text{opt}}\}_1^M$  are rank-1: this result is to be expected as the AN needs to be concentrated solely towards the Eve. Given the previous considerations we can claim that a transmit waveform originated by the solution of problem (15) constitutes an optimal of problem (14), thus making the relaxation tight.

### C. Artificial noise characterization

It can be seen that the AN covariance matrix  $\mathbf{R}_{\Xi_m}$  is used both in the UE SINR and in the Eve SNR definitions. In both equations,  $\mathbf{R}_{\Xi_m}$  appears in the denominator, either multiplied by the communication channel vector  $\mathbf{h}_{m,k}$  or the steering vector  $\mathbf{a}(\theta_m)$ . The latter multiplication inevitably gives  $\mathbf{R}_{\Xi_m}$  a directional selectivity, as shown in Fig. 5

The AN beam pattern peaks around  $\theta_m$  with a rather narrow beamwidth and is otherwise well below 0 dB, in line with the fact that  $\mathbf{R}_{\Xi_m}$  is rank-1. Furthermore, We see that the power beamformed toward the target by AP 2 is lower than its counterpart, this means that the CPU is able to adapt the AN power between APs. Another manifestation of the previously mentioned performance tradeoff can be seen in Fig. 6, where it's shown that an increase in  $\gamma$  corresponds to a decrease in the AN peak value. A possible explanation for this is that as the system tries to guarantee a higher SINR to its users, the

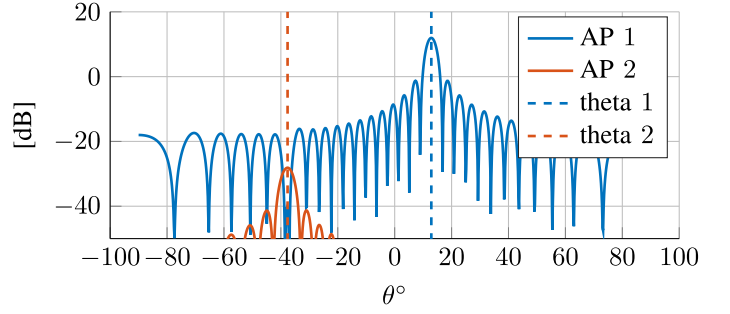


Fig. 5: optimal AN beampattern obtained for  $\gamma = 4$

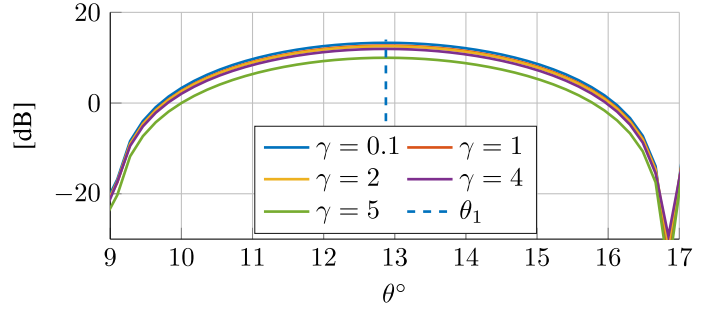


Fig. 6: AP 1's optimal AN beampattern for different values of  $\gamma$

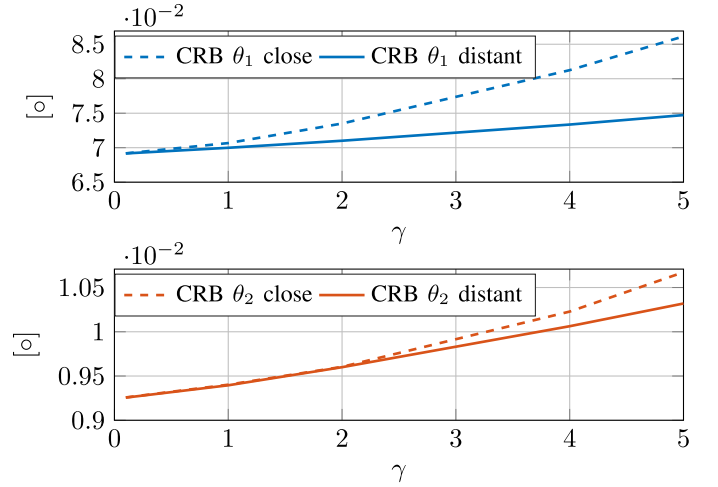


Fig. 7: AP 1 (top) and AP 2 (bottom) CRB on  $\theta_m$  vs  $\gamma$  for different UEs-Eve proximity conditions

term  $|\mathbf{h}_{m,k}^H \mathbf{R}_{\Xi_m} \mathbf{h}_{m,k}|$  must be lower, leading to a progressive decrease of the beampattern peak.

### D. CRB vs SINR and proximity

Fig. 7, two curves are shown, labeled "distant" and "close", respectively. (The "distant" configuration is shown in Fig. 2.) The "close" configuration was created by placing two of the UEs at a distance of 0.5 m from the target, one on the left and one on the right. This configuration has been considered to investigate how the optimization problem would change if one or more UEs angular coordinates would fall within

the AN main lobe depicted in Fig. 5. Fig. 7 confirms the logical intuition that such a proximity between the Eve and one or more UE would inevitably lead to a degradation of the optimization function value. It is also interesting to note that the CRB's proximity-induced degradation is proportional to  $\gamma$ . This behavior can be intuitively attributed to the fact that the system can allocate more resources to the Eve when  $\gamma$  is small, effectively mitigating the disadvantage of proximity. However, when  $\gamma$  becomes larger, the SINR constraint becomes tighter and the system can no longer allocate additional resources to compensate for the proximity, resulting in a higher CRB.

## V. CONCLUSIONS

In this paper, we have considered a secure transmit waveform design used by ISAC APs in a cell-free MIMO environment to serve the communication users while preventing an Eve from spoofing the communication information. To do this, the transmitted dual waveform includes an AN vector whose goal is to degrade the Eve's SNR. The optimal precoding and AN covariance matrices are computed by minimizing the CRB on the monostatic observation angles under SINR constraints for the communication users and maximum SNR constraint for the Eve. Our simulations have shown the inherent tradeoff between sensing and communication performances and how, given the angular directionality of the AN, UEs-Eve proximity degrade the system's performances, making this design strategy very efficient in limiting the impact of an Eve that's physically separated from the legitimate communication users.

## APPENDIX

Here we show how the FIM elements can be expressed as a function of the SDP variable  $\mathbf{W}_s$ :

$$\left( \frac{\partial \mathbf{g}_{m,s}^t}{\partial \Re\{\alpha_{m'}^{m'}\}} \right)^H \frac{\partial \mathbf{g}_{m,s}^t}{\partial \Re\{\alpha_m^{m'}\}} = \quad (17)$$

$$(\phi_{m',s}^t)^H \mathbf{a}(\theta_{m'}) \mathbf{a}(\theta_m)^H \mathbf{a}(\theta_m) \mathbf{a}(\theta_{m'})^H \phi_{m',s}^t = \quad (18)$$

$$N \text{Tr}((\phi_{m',s}^t)^H \phi_{m',s}^t \mathbf{a}(\theta_{m'}) \mathbf{a}(\theta_{m'})^H) \stackrel{(a)}{=} \quad (19)$$

$$N < (\mathbf{W}_{m',s} + \mathbf{R}_{\Xi_{m'}}); \mathbf{a}(\theta_{m'}) >, \quad (20)$$

where in (a) We have used the uncorrelation between the components of  $\phi_{m',s}^t$ , as shown in section II. Let us now move on and present the second type of product

$$\left( \frac{\partial \mathbf{g}_{m,s}^t}{\partial \Re\{\alpha_{m'}^{m'}\}} \right)^H \frac{\partial \mathbf{g}_{m,s}^t}{\partial \theta_m} = \quad (21)$$

$$(\phi_{m',s}^t)^H \mathbf{a}(\theta_{m'}) \mathbf{a}(\theta_m)^H \left[ \alpha_m^{m'} \dot{\mathbf{a}}(\theta_m) \dot{\mathbf{a}}(\theta_m)^H \phi_{m,s}^t + \sum_{\substack{m' \neq m \\ m=1}}^M \alpha_{m'}^{m'} \dot{\mathbf{a}}(\theta_m) \mathbf{a}(\theta_{m'})^H \phi_{m',s}^t \right] = \quad (22)$$

$$(\phi_{m',s}^t)^H \mathbf{a}(\theta_{m'}) \mathbf{a}(\theta_m)^H \alpha_{m'}^{m'} \dot{\mathbf{a}}(\theta_m) \mathbf{a}(\theta_{m'})^H \phi_{m',s}^t = \quad (23)$$

$$\alpha_m^{m'} \text{Tr}((\mathbf{W}_{m',s} + \mathbf{R}_{\Xi_{m'}}) \mathbf{a}(\theta_{m'}) \mathbf{a}(\theta_m)^H \dot{\mathbf{a}}(\theta_m) \dot{\mathbf{a}}(\theta_{m'})^H) \quad (24)$$

where we use the fact that  $\mathbb{E}[(x_{m,s}^t)^H (x_{m',s'}^t)] = 0$  if  $m \neq m'$  and  $\tilde{\mathbf{a}}(\cdot)$  is equal to  $\dot{\mathbf{a}}(\cdot)$  if  $m' = m$  and  $\mathbf{a}(\cdot)$  otherwise.

$$\left( \frac{\partial \mathbf{g}_{m,s}^t}{\partial \theta_m} \right)^H \frac{\partial \mathbf{g}_{m,s}^t}{\partial \theta_m} = \quad (25)$$

$$\left[ \alpha_m^{m'} \dot{\mathbf{a}}(\theta_m) \dot{\mathbf{a}}(\theta_m)^H \phi_{m,s}^t + \sum_{\substack{m' \neq m \\ m=1}}^M \alpha_{m'}^{m'} \dot{\mathbf{a}}(\theta_m) \mathbf{a}(\theta_{m'})^H \phi_{m',s}^t \right]^H \left[ \alpha_m^{m'} \dot{\mathbf{a}}(\theta_m) \dot{\mathbf{a}}(\theta_m)^H \phi_{m,s}^t + \sum_{\substack{m' \neq m \\ m=1}}^M \alpha_{m'}^{m'} \dot{\mathbf{a}}(\theta_m) \mathbf{a}(\theta_{m'})^H \phi_{m',s}^t \right] = \quad (26)$$

$$|\alpha_m^{m'}|^2 \text{Tr}((\mathbf{W}_{m,s} + \mathbf{R}_{\Xi_m}) \dot{\mathbf{a}}(\theta_m) \dot{\mathbf{a}}(\theta_m)^H \dot{\mathbf{a}}(\theta_m) \dot{\mathbf{a}}(\theta_m)^H) + |\alpha_{m'}^{m'}|^2 \text{Tr}((\mathbf{W}_{m',s} + \mathbf{R}_{\Xi_{m'}}) \mathbf{a}(\theta_{m'}) \dot{\mathbf{a}}(\theta_m)^H \dot{\mathbf{a}}(\theta_m) \mathbf{a}(\theta_{m'})^H) \quad (27)$$

where  $\dot{\mathbf{a}}(\cdot)$  is the steering vector's first derivative, defined as  $[\dot{\mathbf{a}}(\theta_m)]_n = j\pi n \cos(\theta_m) e^{j\pi n \sin(\theta_m)}$ . All the other kind of products appearing in the FIM have been omitted due to space constraints.

## REFERENCES

- [1] F. Liu, Y. Cui, C. Masouros, J. Xu, T. X. Han, Y. C. Eldar, and S. Buzzi, "Integrated sensing and communications: Towards dual-functional wireless networks for 6g and beyond," *IEEE journal on selected areas in communications*, 2022.
- [2] J. M. Mateos-Ramos, C. Häger, M. F. Keskin, L. L. Magoarou, and H. Wymeersch, "Model-driven end-to-end learning for integrated sensing and communication," *arXiv preprint arXiv:2212.10211*, 2022.
- [3] Z. Behdad, Ö. T. Demir, K. W. Sung, E. Björnson, and C. Cavdar, "Power allocation for joint communication and sensing in cell-free massive mimo," in *GLOBECOM 2022-2022 IEEE Global Communications Conference*. IEEE, 2022, pp. 4081–4086.
- [4] Y. Liu, Z. Qin, M. El-kashlan, Y. Gao, and L. Hanzo, "Enhancing the physical layer security of non-orthogonal multiple access in large-scale networks," *IEEE Transactions on Wireless Communications*, vol. 16, no. 3, pp. 1656–1672, 2017.
- [5] S. Shi, Z. Wang, Z. He, and Z. Cheng, "Constrained waveform design for dual-functional mimo radar-communication system," *Signal Processing*, vol. 171, p. 107530, 2020.
- [6] R. Melki, H. N. Noura, M. M. Mansour, and A. Chehab, "A survey on ofdm physical layer security," *Physical Communication*, vol. 32, pp. 1–30, 2019.
- [7] U. Demirhan and A. Alkhateeb, "Cell-free isac mimo systems: Joint sensing and communication beamforming," *arXiv preprint arXiv:2301.11328*, 2023.
- [8] N. Su, F. Liu, and C. Masouros, "Sensing-assisted eavesdropper estimation: An isac breakthrough in physical layer security," *arXiv preprint arXiv:2210.08286*, 2022.
- [9] P. Zhang, Y. Jiang, C. Lin, Y. Fan, and X. Shen, "P-coding: secure network coding against eavesdropping attacks," in *2010 Proceedings IEEE INFOCOM*. IEEE, 2010, pp. 1–9.
- [10] X. Liu, T. Huang, N. Shlezinger, Y. Liu, J. Zhou, and Y. C. Eldar, "Joint transmit beamforming for multiuser mimo communications and mimo radar," *IEEE Transactions on Signal Processing*, vol. 68, pp. 3929–3944, 2020.
- [11] A. Zahernia, M. J. Dehghani, and R. Javidan, "Music algorithm for doa estimation using mimo arrays," in *2011 6th International Conference on Telecommunication Systems, Services, and Applications (TSSA)*. IEEE, 2011, pp. 149–153.
- [12] A. B. Gershman, N. D. Sidiropoulos, S. Shahbazpanahi, M. Bengtsson, and B. Ottersten, "Convex optimization-based beamforming," *IEEE Signal Processing Magazine*, vol. 27, no. 3, pp. 62–75, 2010.
- [13] Z.-Q. Luo, W.-K. Ma, A. M.-C. So, Y. Ye, and S. Zhang, "Semidefinite relaxation of quadratic optimization problems," *IEEE Signal Processing Magazine*, vol. 27, no. 3, pp. 20–34, 2010.